

D005

## Pore Fluid Effects on Seismic P- and S-wave Attenuation in Rocks with Double Porosity and Patchy Saturation

B. Quintal\* (ETH Zurich), H. Steeb (Ruhr-University Bochum), M. Frehner (University of Vienna) & S.M. Schmalholz (University of Lausanne)

### SUMMARY

---

Biot's equations of consolidation are numerically solved to yield the stress-strain relations, used to calculate the complex moduli of 2D poroelastic media with mesoscopic-scale heterogeneities. With these moduli, attenuation caused by the mechanism of wave-induced fluid flow is determined. In our models, rocks are represented by media containing circular heterogeneities of much lower porosity and permeability than the background. The background contains 80% of the total porous space in the medium and is fully saturated with oil, gas, or water, while the heterogeneities are always fully saturated with water. We observe that, at low seismic frequencies (1-20 Hz), the P-wave attenuation can be very high in the medium saturated with 80% of oil or gas. The S-wave attenuation in the medium with 80% of oil is much higher than in the one with 80% of gas. At very low frequencies (1 Hz), the S-wave attenuation in the medium with 80% of oil is also much higher than in the one with 100% of water. This occurs because the maximum value of the S-wave attenuation is shifted to lower frequencies with increasing fluid viscosity. Numerical and laboratory experiments can be used to establish patterns for these relationships.

## Introduction

Attenuation of seismic waves in partially saturated, porous rocks is of great interest because it has been observed that oil and gas reservoirs frequently exhibit high attenuation, especially at low seismic frequencies (Chapman et al. 2006). At low seismic frequencies, wave-induced fluid flow caused by fluid pressure differences between mesoscopic-scale heterogeneities is a major cause of P-wave attenuation in a partially saturated porous rock (e.g., White 1975; Pride et al. 2004; Müller et al. 2010). The mesoscopic scale is the scale much larger than the pore size, but much smaller than the wavelength. A partially saturated rock is approximated as a patchy saturated poroelastic medium, that is, a medium with regions fully saturated by one fluid and other regions fully saturated by another fluid. Mesoscopic-scale heterogeneities can also occur in the solid frame properties by the so-called double-porosity model. In this paper, we study P- and S-wave attenuation in partially saturated media of heterogeneous solid frame by introducing double porosity and patchy saturation in our models. We focus on fluid effects for P- and S-wave attenuation. Because we consider commercial hydrocarbon reservoirs as the potential application of this study, we compare media with varying saturation: (1) 80% of oil, 20% of water; (2) 80% of gas, 20% of water; and (3) 100% of water.

## Methodology

We use the finite element method to solve Biot's equations of consolidation (Biot 1941) in the displacement-pressure (u-p) formulation. We perform 2D quasi-static creep tests on poroelastic media with mesoscopic-scale heterogeneities to calculate the complex moduli from the modeled stress-strain relations. From the complex moduli, we calculate the frequency-dependent attenuation caused by fluid flow induced by pressure differences between regions of different compliances due to contrasts in fluid and/or solid frame properties. The numerical simulation is performed on the Representative Elementary Volume (REV) of the medium. The REV is a 40-cm side square and the radius of the circular heterogeneity is 16 cm. The circle occupies 50% of the REV. The algorithm employs an unstructured mesh, shown in Figure 1, which makes it accurate for simulations in media with heterogeneities of arbitrary geometries. Additionally, it employs variable time stepping, shown in Figure 2, which makes it very efficient. Small steps at the beginning are necessary to accurately resolve the high frequencies. For a detailed description of the algorithm, refer to Quintal et al. (2011).

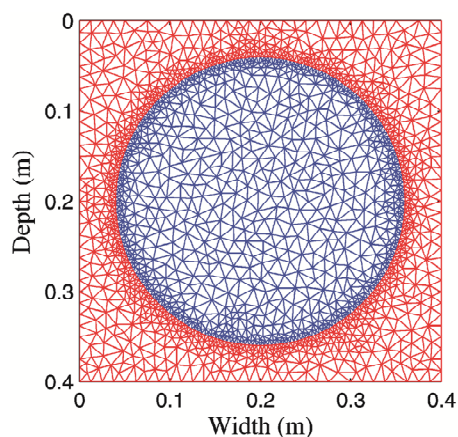


**Figure 1.** Unstructured finite element mesh of the REV (Delauney triangulation) (Shewchuk 2002). Each triangular element (quadratic-shape functions) consists of seven nodal points, on which the solid displacements and fluid pressure are calculated. Blue and red lines are used for the mesh inside and outside the patch where the elements have different petrophysical properties. The spatial resolution of the mesh can strongly vary.

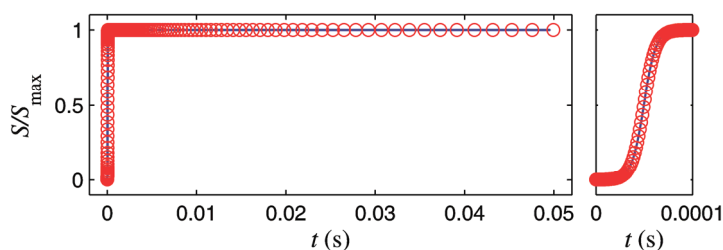


**Figure 2.** Time function, normalized by its maximum value, with variable time steps (red circles). Increments are constant during 0.1% of the total time, and linearly increased with time afterwards. A zoom into the first steps is shown on the right.

To calculate both S- and P-wave attenuation from a single numerical simulation, we model a biaxial compression test by applying normal compressive stresses of different magnitudes vertically,  $4S(t)$ , and horizontally,  $3S(t)$ , on the boundaries. The evolution of the boundary conditions,  $S(t)$ , is shown in Figure 2. With the stress and strain rates obtained from the experiment, we calculate the undrained bulk modulus,  $K$ , and the undrained shear modulus,  $\mu$ , using equations D3 and D4 from Quintal et al. (2011). The moduli  $K$  and  $\mu$  are used to calculate the P- and S-wave quality factors with the formulas given in Table 1. The inverse of quality factor is a measure of attenuation. In Figure 3 we show a test of the numerical scheme by comparing its result for the real part of the P-wave modulus,  $H$  (Table 1), in the low- and high-frequency limits with theoretically predicted values.

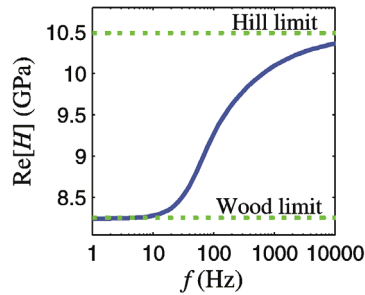


**Figure 3.** Test of the numerical scheme for the real part of the P-wave modulus,  $H$ , in a patchy saturated medium of homogeneous solid frame. The background is saturated with gas and the circular patch (Figure 1) with water. The properties of the fluids are given in Table 2, and the properties of the solid frame are  $K_d = 4$  GPa,  $\mu_d = 3$  GPa, and  $\rho_s$ ,  $K_s$ ,  $\phi$  and  $k$  given in Table 3. The symbols are defined in Table 1. The low- and high-frequency limits of  $Re[H]$  fit the theoretical Gassmann-Wood and -Hill limits (Mavko et al. 1998).

## Simulations

Our main purpose is to evaluate fluid effects on P- and S-wave attenuation in rocks with heterogeneous solid frame. The model consists of mesoscopic-scale circular heterogeneities characterized by low permeability and low porosity, embedded in a background medium of high permeability and high porosity. Because of the different porosities of the heterogeneity and of the background (Table 3), the porous space in the background corresponds to 80% of the total porous space in the medium. The heterogeneities are always fully saturated with water, and the background is fully saturated with oil, gas, or water (Table 2). Three degrees of saturation are studied: (1)  $S_o = 80\%$  and  $S_w = 20\%$ ; (2)  $S_g = 80\%$  and  $S_w = 20\%$ ; and (3)  $S_w = 100\%$ ; where  $S_o$ ,  $S_g$ , and  $S_w$  denote saturation of oil, gas, and water, respectively. Additionally, we consider two distributions of rock frame properties described in Table 3: in Case A, the heterogeneity is more compliant than the background; in Case B, the background is the most compliant. The results for the real part of the P-wave modulus,  $H$ , the P-wave attenuation,  $1/Q_P$ , the real part of the undrained shear modulus,  $\mu$ , and the S-wave attenuation,  $1/Q_S$ , are shown in Figures 4 and 5. Formulas for  $H$ ,  $Q_P$ , and  $Q_S$  are given in Table 1.

**Table 1.** Symbols.

$\rho_f$	Density of the fluid
$\eta$	Viscosity of the fluid
$K_f$	Bulk modulus of the fluid
$\rho_s$	Density of the grains
$K_s$	Bulk modulus of the grains
$\phi$	Porosity
$k$	Permeability
$K_d$	Bulk modulus of the dry frame
$\mu_d$	Shear modulus of the dry frame
$K$	Undrained bulk modulus
$\mu$	Undrained shear modulus
$H$	P-wave modulus $= K + (4/3)\mu$
$Q_P$	P-wave quality factor $= Re[H]/Im[H]$
$Q_S$	S-wave quality factor $= Re[\mu]/Im[\mu]$

**Table 2.** Physical properties of the fluids.

Fluid	Water	Oil	Gas
$\rho_f$ (kg/m <sup>3</sup> )	1010	700	160
$\eta$ (Pa s)	0.003	0.1	$2 \times 10^{-5}$
$K_f$ (GPa)	2.4	0.7	0.04

**Table 3.** Physical properties of the solid frame.

Region	Heterogeneity	Background
$\rho_s$ (kg/m <sup>3</sup> )	2700	2700
$K_s$ (GPa)	40	40
$\phi$ (%)	7	25
$k$ (mD)	100	1000
Case A	More compliant	Less compliant
$K_d$ (GPa)	4	12
$\mu_d$ (GPa)	3	11
Case B	Less compliant	More compliant
$K_d$ (GPa)	12	4
$\mu_d$ (GPa)	11	3

## Results

At the low-frequency (quasi-static) limit, our results (Figures 4 and 5) agree with a prediction of Gassmann's (1951) theory that the undrained shear modulus,  $\mu$ , is independent on the properties of the saturating fluid. For higher frequencies, the value of  $\mu$  in our results changes with changing fluid saturation, which is predicted by Berryman and Wang (2001) by applying the effective-medium theory to poroelastic media of heterogeneous solid frame.

In Figure 4 we observe that the P-wave attenuation can be very high in the media with  $S_o = 80\%$  and  $S_g = 80\%$ , but it can be also significant in the medium with  $S_w = 100\%$ . The minimum values of  $Q_P$ , equivalent to maximum values of P-wave attenuation, are: 9.2 at 7.4 Hz for  $S_o = 80\%$ ; 6.4 at 13.4 Hz for  $S_g = 80\%$ ; and 23.4 at 25.7 Hz for  $S_w = 100\%$ . The respective maximum values of S-wave attenuation are more than one order of magnitude lower than those of P-wave attenuation. In Figure 5, compared to Figure 4, the P-wave attenuation is not so high, with minimum values of  $Q_P$ : 72.9 at 7.9 Hz for  $S_o = 80\%$ ; 27.6 at 19.4 Hz for  $S_g = 80\%$ ; and 147 at 42.7 Hz for  $S_w = 100\%$ . But the maximum values of S-wave attenuation in the media with  $S_o = 80\%$  and  $S_w = 100\%$  are higher than the respective maximum values of P-wave attenuation. In the medium with  $S_g = 80\%$ , as in Figure 4, the maximum value of S-wave attenuation is much lower than the one of P-wave attenuation.

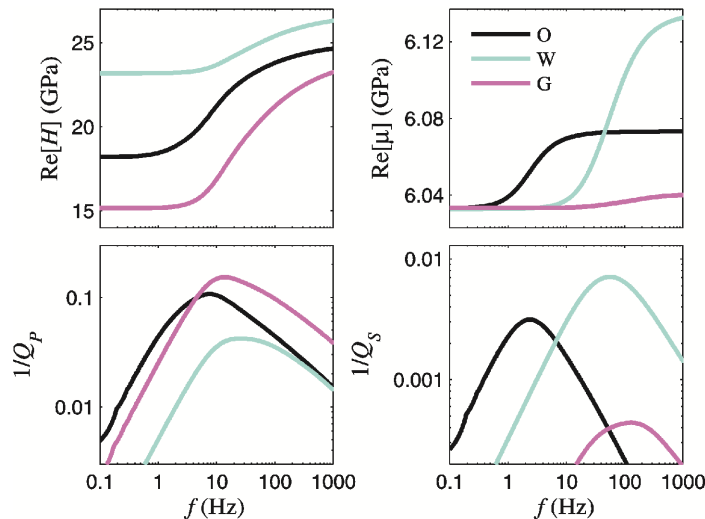


**Figure 4.** Numerical results for the real part of the P-wave modulus,  $H$ , the P-wave attenuation,  $1/Q_P$ , the real part of the undrained shear modulus,  $\mu$ , and the S-wave attenuation,  $1/Q_S$ , when the heterogeneity is more compliant than the background (Case A). The legend terms refer to the background saturated with oil (O), gas (G), or water (W). In this order, at 1 Hz, the values of  $Q_P$  are 21.8, 37.4, and 188, and the values of  $Q_S$  are 426, 6412, and 2937.

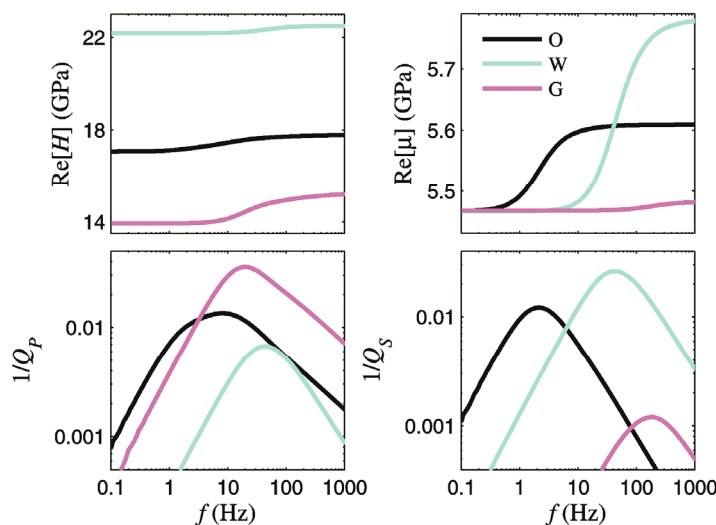


**Figure 5.** Numerical results for the real part of the P-wave modulus,  $H$ , the P-wave attenuation,  $1/Q_P$ , the real part of the undrained shear modulus,  $\mu$ , and the S-wave attenuation,  $1/Q_S$ , when the background is more compliant than the heterogeneity (Case B). The legend terms refer to the background saturated with oil (O), gas (G), or water (W). In this order, at 1 Hz, the values of  $Q_P$  are 137, 251, and 2906, and the values of  $Q_S$  are 102, 5792, and 737.

In both Figures 4 and 5, from 1 to 20 Hz: the P-wave attenuation can be very high in the media with  $S_o = 80\%$  and  $S_g = 80\%$ , and is significantly higher than in the fully water-saturated media; and the S-wave attenuation is much higher in the medium with  $S_o = 80\%$  than in the one with  $S_g = 80\%$ .

Although the maximum values of S-wave attenuation in the media with  $S_w = 100\%$  are higher than the ones in the media with  $S_o = 80\%$ , at 1 Hz, the S-wave attenuation is significantly higher for  $S_o = 80\%$ . This occurs because the maximum value of S-wave attenuation is shifted to lower frequencies with increasing fluid viscosity. The values for  $Q_P$  and  $Q_S$  at 1 Hz are given in the captions of Figures 4 and 5. In both figures, at 1 Hz, the S-wave attenuation in the media with  $S_o = 80\%$  is about 7 times higher than in the one with  $S_w = 100\%$ , and it is close to zero ( $Q_S > 5000$ ) in the medium with  $S_g = 80\%$ .

## Discussion and conclusions

It is well known that in White's model, a medium of homogeneous frame, partially (patchy) saturated with water and gas, exhibits high P-wave attenuation when it has a low gas saturation of around 10% (e.g., Quintal et al. 2009). However, when the medium has a heterogeneous frame, in addition to patchy saturation, more parameters rule the compressibility and fluid mobility ( $k/\eta$ ) in the different regions, and the P-wave attenuation can be very high for large oil or gas saturations, as in Figure 4.

We suggest that the relationships among attenuation values in rocks differing in fluid saturation can help extract fluid information from seismic data. Numerical and laboratory experiments can be used to establish patterns for these relationships. For example, as observed in Figures 4 and 5 at very low frequencies (1 Hz), the S-wave attenuation is much higher in a medium of heterogeneous solid frame when it is mostly saturated with oil than when it is mostly saturated with gas or with 100% of water.

## Acknowledgements

This work is supported by Spectraseis and the Low Frequency Seismic Partnership (LFSP). B. Quintal thanks Marc-André Lambert for stimulating discussions, and Erik Saenger, Brad Artman, and Rob Habiger for helpful suggestions.

## References

- Berryman, J.B., and Wang, H.F. [2001] Dispersion in poroelastic systems. *Phys. Rev. E*, **64**, 011303.
- Biot, M.A. [1941] General theory of three-dimensional consolidation. *J. App. Phys.*, **12**, 155-164.
- Chapman, M., Liu, E. and Li, X. [2006] The influence of fluid-sensitive dispersion and attenuation on AVO analysis. *Geophys. J. Int.*, **167**, 89-105.
- Gassmann, F. [1951] Über die Elastizität poröser Medien. *Vierteljahrsschrift der Naturforschenden Gesellschaft in Zürich*, **96**, 1-23.
- Mavko, G., Mukerji, T. and Dvorkin, J. [1998] The rock physics handbook: Tools for seismic analysis in porous media. Cambridge University Press.
- Müller, T.M., Gurevich, B. and Lebedev, M. [2010] Seismic wave attenuation and dispersion resulting from wave-induced flow in porous rocks – A review. *Geophysics*, **75**, A147-A164.
- Pride, S.R., Berryman, J.G. and Harris, J.M. [2004] Seismic attenuation due to wave-induced flow. *J. Geophys. Res.*, **109**, B01201.
- Quintal, B., Schmalholz, S.M. and Podladchikov, Y.Y. [2009] Low-frequency reflections from a thin layer with high attenuation caused by interlayer flow. *Geophysics*, **74**, N15-N23.
- Quintal, B., Steeb, H., Frehner, M. and Schmalholz, S.M. [2011] Quasi-static finite element modeling of seismic attenuation and dispersion due to wave-induced fluid flow in poroelastic media. *J. Geophys. Res.*, **116**, B01201.
- Shewchuk, J.R. [2002] Delaunay refinement algorithms for triangular mesh generation. *Comput. Geom.*, **22**, 21-74.
- White, J.E. [1975] Computed seismic speeds and attenuation in rocks with partial gas saturation. *Geophysics*, **40**, 224-232.